RESEARCH ARTICLE

Assessment of Radio Frequency Electromagnetic Field Exposure Induced by Base Stations in Several Micro-Environments in France

WASSIM BEN CHIKHA[1], (Senior Member, IEEE), **YARUI ZHANG**[1], **JIANG LIU**[1], **SHANSHAN WANG**[2], (Member, IEEE), **SRIKUMAR SANDEEP**[1], **MÒNICA GUXENS**[3,4,5,6,7], **ADRIANA FERNANDES VELUDO**[8,9], **MARTIN RÖÖSLI**[8,9], **WOUT JOSEPH**[10], (Senior Member, IEEE), AND **JOE WIART**[1], (Senior Member, IEEE)

[1]Télécom Paris, Institut Polytechnique de Paris, 91120 Palaiseau, France
[2]ETIS, UMR 8051, ENSEA, CNRS, CY Cergy Paris Université, 95000 Paris, France
[3]ISGlobal, 08036 Barcelona, Spain
[4]Universitat Pompeu Fabra, 08002 Barcelona, Spain
[5]Spanish Consortium for Research on Epidemiology and Public Health (CIBERESP), 28029 Madrid, Spain
[6]Instituto de Salud Carlos III, 28029 Madrid, Spain
[7]Department of Child and Adolescent Psychiatry/Psychology, Erasmus MC, University Medical Centre, 3015 GD Rotterdam, The Netherlands
[8]Department of Epidemiology and Public Health, Swiss Tropical and Public Health Institute, 4123 Allschwil, Switzerland
[9]University of Basel, 4001 Basel, Switzerland
[10]Department of Information Technology, IMEC, Ghent University, 9000 Ghent, Belgium

Corresponding author: Wassim Ben Chikha (wassim.benchikha@telecom-paris.fr)

ABSTRACT Recently, the monitoring of the radiofrequency electromagnetic field (RF-EMF) exposure induced by cellular networks has received a great deal of attention. In this work, a set of 70 microenvironments (MEs) located in urban and rural areas are selected in France under, on the one hand, the French Beyond5G project, and on the other hand, the 5G expOsure, causaL effects and rIsk perception through citizen engagement (GOLIAT) EU project. The purpose of this study is to assess the RF-EMF DL exposure in residential areas, downtowns, business areas, train stations, and public transport rides. For that, we employ the personal ExpoM-RF4 dosimeter placed inside a backpack to perform the measurements in different MEs. To take into consideration the effect of the presence of the human body near the dosimeter, we propose a correction approach that is mainly based on comparing the measurements given by ExpoM-RF4 to the ones provided by a reference system using the Tektronix real-time spectrum analyzer (RTSA) far from the body. Then, we use metrics, such as the quadratic mean, standard deviation, and median of the electric (E) field to carry out a comparative study between different MEs with different RF bands. It was found that the RF-EMF exposure levels for all MEs are well below the maximum allowable exposure limit prescribed by the International Commission on Non-Ionizing Radiation Protection (ICNIRP). In addition, we perform clustering analyses using the K-Means technique to group the MEs with comparable exposure levels. The results show that the exposure level is low, but generally higher in MEs located in Paris than in the other considered areas (i.e., Massy and three villages, namely Igny, Bures-sur-Yvette and Gif-Sur-Yvette). For example, we observe that outdoor MEs can be grouped into three clusters, where the average total E fields (ATEFs) are 0.77 V/m, 0.35 V/m, and 0.08 V/m for the MEs belonging to the first, second and third clusters, respectively. Note that the first cluster here mainly contains the MEs located in Paris. This can be explained by the important number of antennas deployed in that area to serve the huge amount of users. We also observe few locations with exceptions confirming the presence of heterogeneous environments in the vicinity of some areas. For instance, three MEs in Paris among fifteen have an exposure level similar to Massy MEs in outdoor

The associate editor coordinating the review of this manuscript and approving it for publication was Sandra Costanzo.

areas. The clustering of MEs located in transport station, and moving transport also show similar results. Finally, we see that the ATEF in a shopping center and a university in Paris have the highest exposure values comparing to others located in Massy and villages. This also due to the considerable number of deployed antennas in Paris.

INDEX TERMS RF-EMF down link exposure, radiofrequency, k-means clustering technique.

I. INTRODUCTION

Wireless technologies have undergone significant development, driven by increasingly demanding users in terms of throughput and quality of service [1]. This development has been ongoing since the 90s, and is associated with the widespread deployment of base stations [2]. The cellular infrastructures enable the target performance to be achieved, thanks to the emission of RF electromagnetic fields over various frequency bands and the evolution of communication protocols (2G, 3G, 4G and 5G). Despite such a massive use of mobile phones (e.g. in France 87% of the 12 years old are using mobile phones [3], [4], risks perception have arisen, linked to the potential negative impact on human health of exposure to RF-EMFs [5], [6], [7]. This is despite existing protective limits that have been established by the International Commission on Non-Ionizing Radiation Protection (ICNIRP) [8].

Because of the continuous deployment of base station antennas to better serve users and offer a good quality of service, monitoring the exposure linked to RF-EMF is often requested and has therefore been assigned to the objectives of the European Union (EU) call "HORIZON-HLTH-2021-ENVHLTH-02-01" [9]. Four projects have been selected (SEAWave, GOLIAT, ETAIN and nextGEMS) and have, in line with the call, to monitor the RF-EMF exposure induced by cellular networks in the European countries. In GOLIAT [10], MEs in various areas were defined in many European countries to characterize the RF-EMF exposure. They are selected based on population density, and activity of cellular network. This is also in line with the objective of the world health organization (WHO) which encourages the characterization of human exposure to RF-EMFs in different countries [11]. For each ME, the ExpoM-RF4 [12] personal dosimeter is used to measure to RF in terms of electric (E) field. The portable device realizes almost continuous monitoring (sampling time is 6.1s) of RF-EMFs in different frequency bands, including 700, 800, 900, 1800, 2100, 2600, and 3500 MHz. However, dosimeter measurements are affected by the presence of the experimenter's body [13], [14]. In fact, instead of measuring the actual incident fields, the dosimeter allows measuring the electric fields affected by the presence of the body and consequently leads to uncertainties in measuring the actual incident fields. For that reason, several experiments are carried out to address this issue by performing on-body calibration of dosimeters [15], [16], [17]. For example, in [18], the authors have proposed a multi-band body-worn distributed exposure meter for simultaneous measurement of the incident power density in 11 frequency bands, where on-body calibration is done inside an anechoic chamber in order to improve the measurement accuracy of incident RF-EMFs on-body. This kind of calibration has demonstrated its effectiveness in outdoor environments, where the incident fields can be seen as specular components [19].

To the best of the authors' knowledge, this paper presents, for the first time, an EMF DL exposure assessment study in 70 MEs in France located in five areas of interest based on population density and and activity of cellular network. It includes one large city, one smaller city, and three villages in rural areas. The goal is to assess EMF Down Link (DL) exposure (i.e., the EMF field emitted by base station and used to link the base station antenna and mobile antenna) coming from residential areas, downtowns, business areas, train stations, and public transport rides in these five areas. To this end and following the GOLIAT protocol, we use the personal ExpoM-RF4 dosimeter hold in a backpack to carry out the measurements in different MEs. This way of holding the ExpoM-RF4 requires taking into consideration the effect of the presence of the human body near the dosimeter that obviously affects the antenna pattern and the Antenna Factor [20], [21]. Then, we propose a correction approach that is mainly based on comparing the measurements given by ExpoM-RF4 to the ones provided by a reference system using the Tektronix RTSA [22] far from the body. This approach allows to determine the correction coefficients for each frequency band. Thereafter, we apply the corresponding correction factor to the total number of measurements in all MEs. Statistical analyses, using quadratic mean, standard deviation and median of the E field are used to carry out a comparative study between different MEs with different RF bands. We also perform clustering analyses using the K-Means technique to group the MEs with comparable exposure levels.

The remainder of this paper is organized as follows. First, we describe the selected MEs in France in Section II. In section III, we present the proposed ExpoM-RF4 correction approach followed by clustering analysis using the K-Means technique is carried out to group the MEs with comparable exposure levels. Finally, in Section IV, we conclude the paper with some discussions.

II. SELECTED MICRO-ENVIRONMENT IN FRANCE

As explained in the introduction, ExpoM-RF4 [12] is used as a personal dosimeter to assess RF-EMF exposure from legacy, current, and newly introduced technologies. For

TABLE 1. Description of each ME in the largest city "Paris", secondary city "Massy" and Villages "Gif-Sur-Yvette", "Bures-Sur-Yvette" and "Igny."

MEs					Descriptions
ME1_P	ME1_M	N/A	N/A	N/A	1st downtown area
ME2_P	N/A	N/A	N/A	N/A	2nd downtown area
ME3_P	ME2_M	N/A	N/A	N/A	Business area
N/A	ME3_M	N/A	N/A	N/A	Industrial area
N/A	N/A	ME1_G	ME1_B	ME1_I	Village centre
ME4_P	ME4_M	ME2_G	ME2_B	ME2_I	1st Residential area: central
ME5_P	ME5_M	N/A	N/A	N/A	2nd Residential area: central
ME6_P	N/A	N/A	N/A	N/A	3rd Residential area: central
ME7_P	ME6_M	N/A	N/A	N/A	1st Residential area: non central
ME8_P	ME7_M	N/A	N/A	N/A	2nd Residential area: non central
ME9_P	N/A	N/A	N/A	N/A	3rd Residential area: non central
ME10_P	ME8_M	N/A	N/A	N/A	1st Residential area: outskirts
ME11_P	ME9_M	N/A	N/A	N/A	2nd Residential area: outskirts
ME12_P	N/A	N/A	N/A	N/A	3rd Residential area: outskirts
ME13_P	ME10_M	ME3_G	ME3_B	ME3_I	Public park: central
ME14_P	ME11_M	N/A	N/A	N/A	Public park: non central
ME15_P	ME12_M	N/A	N/A	N/A	Public park: outskirts
ME16_P	ME13_M	N/A	N/A	N/A	University
ME17_P	ME14_M	ME4_G	ME4_B	ME4_I	Shopping centre
ME18_P	ME15_M	ME5_G	ME5_B	ME5_I	Bus station: central
ME19_P	ME16_M	N/A	N/A	N/A	Bus station: secondary station
ME20_P	ME17_M	ME6_G	ME6_B	ME6_I	Train station: central station
ME21_P	ME18_M	N/A	N/A	N/A	Train station: secondary station
ME22_P	N/A	N/A	N/A	N/A	Metro station
ME23_P	ME19_M	ME7_G	ME7_B	ME7_I	Bus
ME24_P	ME20_M	ME8_G	ME8_B	ME8_I	Train
ME25_P	N/A	N/A	N/A	N/A	Metro
ME26_P	N/A	N/A	N/A	N/A	Tram

N/A: Not Applicable

that, in EU project GOLIAT [10], small-scale environments are selected from larger environments. We refer to these environments as micro-environments. In such a context, a micro-environment is a residential area, downtown, business area, train station, and public transport ride (e.g., train, bus, tram). In the following, we will describe the selected micro-environments in France. The measurements of this study are carried out by 5 experimenters in walking mode. In total, we considered five study areas based on population density: one large city, one smaller city, and three villages. A total of 70 MEs are selected. For each ME, three scenarios are considered where a mobile phone equipped with an add-on RF-EMF sensor is placed on top of the backpack to mimic the auto-induced exposure caused by one's personal phone. In the following, we describe the considered "non-user" scenario defined in the EU GOLIAT project, where the mobile phone is set to flight mode and consequently we only measure environmental DL and UL exposure not affected by the user's phone.

In this paper, our goal is to characterize the environmental DL exposure in France. The experimenter walks in a specific ME/stays inside a moving means of transport for about 15 minutes. With a standard walk at 3.6 km/h, each route's length is about 1 km.

In Table 1, we present different MEs for the five considered study areas. As seen from those tables, we select Paris and Massy as large and smaller cities, respectively, and Gif-sur-Yvette, Bures-sur-Yvette, and Igny as villages. In this study,

our purpose is to characterize the environmental DL exposure in France with the "non-user" scenario.

III. EXPOSURE ASSESSMENT
A. MEASUREMENT PROTOCOL
Usually, the RF-EMF exposure assessment induced by cellular base stations is often carried out using a spectrum analyzer and a three-axis antenna. Such an approach is accurate but quite difficult in crowded area such as public transportation. In our case, the RF-EMF exposure measurements are conducted using a personal dosimeter held in a backpack. This personal dosimeter performs a frequency-selective analysis using hardware filters. It is placed in a case to prevent movement during the measurements as shown in Figure 1. This case is then packed in a backpack, that is worn while measuring. The dosimeter selected in the GOLIAT project, namely ExpoM-RF4 [12], is used by all the involved partners. The main advantage of this personal dosimeter is its portability. While a spectrum analyzer (SA) such as RTSA from Tektronix [22], based on Fourier transform, allows changing the frequency band analyzed, ExpoM-RF4 is a frequency-selective measurement system based on fixed frequency bandwidth filters of 35, 75 or 100 MHz. Using ExpoM-RF4, data is continuously sampled for the measurement duration of 50 ms per band. Thereafter, the root mean square (RMS) value of the signal is computed by the digital signal processing stage and stored in memory. Accordingly, it has the ability to measure a broad frequency
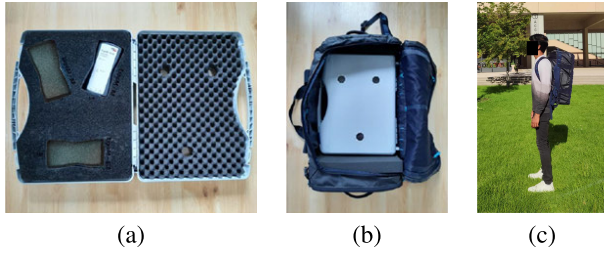
FIGURE 1. Way of holding the dosimeter by the experimenter: (a) placing the dosimeter in a case, (b) packaging the case in a backpack and (c) carrying the backpack.

FIGURE 2. ExpoM-RF4 position relative to the human body.

range from 50 MHz up to 6 GHz and offers the measurement of 35 pre-defined bands used by 2G, 3G, 4G, and 5G technologies for both uplink (UL) and DL. Measurements can be done every 6.1 s including global positioning system (GPS) localization information.

B. ExpoM-RF4 CORRECTION APPROACH CONSIDERING THE HUMAN BODY

The presence of the human body near ExpoM-RF4 affects the antenna pattern as well as the antenna factor [20], [21] and consequently a correction approach is needed to take into account this effect (see Figure 2). To this end, we proposed to carry out measurements along a circle and compare them to reference measurements performed using frequency-selective Tektronix measurements. In Figure 3, we present the details of the used approach for determining the correction coefficients for different frequency bands. In fact, we mount the measurement probe (TAS-1208-01) [23] on a tripod at a height of 1.5 m above the ground. This probe is considered as a measurement system of reference and allows performing RF-EMF measurements on the three orthogonal polarizations (X, Y, and Z) from 9 kHz to 6 GHz. It is connected to a RTSA (RSA306B from Tektronix) [22]. Here, a switch is used to alternate between the different three orthogonal polarizations.
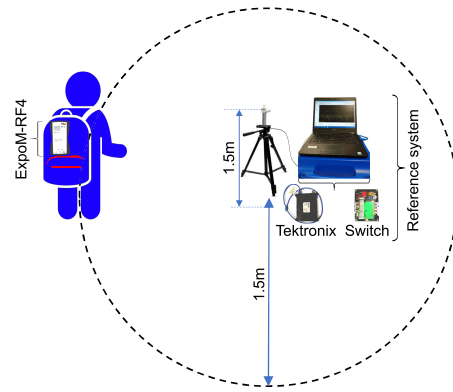

FIGURE 3. Consideration of the presence of the human body for ExpoM-RF4 measurements.

In this work, we configure the Tektronix spectrum analyzer to record the three polarizations over a large frequency band covering 700-3800 MHz that includes all RF bands used by different existing cellular wireless technologies. For this considered wide frequency band, the record of one measurement over the 3-axis using the Tektronix lasts about 0.8 s. For a given DL band f, the resulting isotropic E field strength of the three ports can be expressed as

$$E_f = \sqrt{\sum_{p=1}^{3} E_{f_p}^2}, \qquad (1)$$

where E_{f_p} represents the E field strength at frequency f associated to the port p. After placing the tripod in the center of a circle with a radius of 1.5m and far from the existing base stations, we conducted measurements with seven different experimenters in order to average out the variability of body absorption. Each person wears the backpack containing the ExpoM-RF4 and walks around the reference system for 3 minutes.

Consider N_D the total number of measurements performed by the seven experimenters using the Tektronix (T) or ExpoM-RF4 (E) device (i.e., $D = \{T, E\}$), the correction coefficients for each DL frequency band f is given by

$$\alpha_f = \frac{\mu_{T,f}}{\mu_{E,f}}, \qquad (2)$$

where $\mu_{D,f}$ is the average electric field measured by the device $D = \{T, E\}$ for the frequency band f and given by the quadratic mean of the collected N_D independent samples of electric field strength $E_{n,f}, n = 1, \ldots, N_D$. It is expressed as follows

$$\mu_{D,f} = \sqrt{\frac{\sum_{n=1}^{N_D} \left(E_{n,f}\right)^2}{N_D}}. \qquad (3)$$

In Table 2, we present the correction coefficients α_f and std for different DL bands. All the measurements given by the ExpoM-RF4 are then corrected using those coefficients.

TABLE 2. Correction coefficients and std for different DL bands.

f (MHz)	α_f	Std
700	0.89	0.02
800	1.06	0.16
900	1.08	0.13
1800	0.44	0.40
2100	0.46	0.20
2600	1.31	0.14
3500	0.81	0.40

The results in terms of the average electric field for all MEs and different DL RF bands in V/m using the corrected measurements are summarized in Table 3. We also present the median of the electric field for all MEs and different DL RF bands in V/m after applying the correction coefficients in Table 4. One can clearly see that the maximum average RF-EMF DL exposure levels in all MEs are well below the ICNIRP [8] for all frequencies. For the sake of comprehensive data analysis of the measurements in all studied MEs, we propose to apply the K-Means technique to cluster the MEs with similar exposure levels based on the average E fields summarized in Table 3. To this end, we decided to address separately the following three environmental categories: i) outdoor, ii) transport station, and iii) moving transport. Thus, we will apply the K-Means to determine the clusters presented in the five considered areas for these three environment categories. However, for the shopping centers and universities, we propose to analyze the ATEF in different areas as their numbers are limited (i.e., we have in total 5 shopping centers and 2 universities). In the following, we present the descriptions and results of those analyses.

C. CLUSTERING ANALYSIS USING THE K-MEANS TECHNIQUE

In this study, we adopt the K-means technique [24] to firstly address the clustering of the RF-EMF measurements in 33 outdoor MEs excluding public and transport stations, i.e., ME1_P, ME2_P, ME4_P, ME5_P, ME6_P, ME7_P, ME8_P, ME9_P, ME10_P, ME11_P, ME12_P, ME13_P, ME14_P, ME15_P, ME1_M, ME4_M, ME5_M, ME6_M, ME7_M, ME8_M, ME9_M, ME10_M, ME11_M, ME12_M, ME1_G, ME2_G, ME3_G, ME1_B, ME2_B, ME3_B, ME1_I, ME2_I, ME3_I. The purpose is to determine the study areas that have comparable exposure levels. This technique is computationally efficient compared to Gillespie and Monte Carlo algorithms [25]. Here, we consider a dataset $\mathscr{S}$ containing K 9-dimensional observations. Hence, $\mathscr{S} = \{\mathbf{o}_k \mid k = 1, \ldots, K\}$, where $\mathbf{o}_k =$

$$\left(\underbrace{x_k}_{o_{k1}}, \underbrace{y_k}_{o_{k2}}, \underbrace{m_{k,1}}_{o_{k3}}, \underbrace{m_{k,2}}_{o_{k4}}, \underbrace{m_{k,3}}_{o_{k5}}, \underbrace{m_{k,4}}_{o_{k6}}, \underbrace{m_{k,5}}_{o_{k7}}, \underbrace{m_{k,6}}_{o_{k8}}, \underbrace{m_{k,7}}_{o_{k9}} \right) \in$$

$\mathbb{R}^9$. x_k, y_k, and $m_{k,i}$, $i = \{1, 2, \ldots, 7\}$ are the values of the longitude and latitude of the walked midway for each considered ME and the average of E field for different DL bands 700, 800, 900, 1800, 2100, 2600, and 3500 MHz, respectively. The clustering process aims to group the observations in a dataset $\mathscr{S}$ into a specified number of clusters C, with the goal of maximizing the similarity of observations within each cluster and maximizing the dissimilarity between clusters. This is achieved by iteratively assigning observations to the closest cluster centroids and updating the centroids until their positions remain unchanged. It is worth noting that the complexity of the K-Means is significantly lower compared to the exhaustive search algorithm. We present the K-Means process in Algorithm 5. Its procedure begins by setting the iteration counter $t \leftarrow 1$ randomly choosing a number of C observations from $\mathscr{S}$. Thus, those later are considered as the C initial centroids, denoted by $\mathbf{g}_c$, $c = 1, \ldots, C$. Thereafter, the Euclidean distance is computed in step 2 in order to determine the distance between each observation and the $\mathbf{g}_c$. The distance between two observations $\mathbf{o}^1$ and $\mathbf{o}^2$ is given by

$$d_{\mathbf{o}^1 \mathbf{o}^2} = \sqrt{\sum_{i=1}^{9} \left(o^1_i - o^2_i \right)^2}. \tag{4}$$

Step 3 concerns the assignment of each observation $\mathbf{o}_k$ to the cluster G_c with a centroid nearest to it. Step 4 allows to determine the new centroids of all the C clusters. The K-Means technique is based on an iterative process leading to changing the centroid positions of the C clusters until the convergence is reached or a maximum number of iterations is achieved.

Algorithm 1 Considered K-Means Algorithm

---

inputs　　: Number of clusters: C
　　　　　　 Dataset: $\mathscr{S} = \{\mathbf{o}_k \mid k = 1, \ldots, k\}$
outputs　 : Clusters: G_c, $c = 1, \ldots, C$

1 **init:** Set the iteration counter to 1 (i.e., $t \leftarrow 1$) and randomly choose C observations from $\mathscr{S}$, and using them as initial centroids, denoted by $\mathbf{g}_c$, $c = 1, \ldots, C$.
2 Using (4), compute the Euclidian distance between each observation $\mathbf{o}_k$ and the cluster centroids.
3 Assign each observation $\mathbf{o}_k$ to the cluster whose centroid is the closest to it.
4 Find the new centroids $\mathbf{g}_c$, $c = 1, \ldots, C$ positions of all the C clusters and set $t \leftarrow t + 1$.
5 Repeat steps 2-4 until the convergence is reached or a maximum number of iterations is achieved.

In Figure 4, we present the results of the K-Means clustering using 3 groups. It is seen that the exposure levels in rural environments Gif-Sur-Yvette, Bures-sur-Yvette, and Igny are similar. The two other clusters include MEs from Paris and Massy. The ATEFs are 0.77 V/m, 0.35 V/m, and 0.08 V/m for the MEs belonging to the red, yellow and green clusters, respectively. This can be explained by the number of deployed antennas and the population presented in different areas. One can also see that few locations with exceptions confirming the presence of heterogeneous environments in the vicinity of some areas.

TABLE 3. Average and std of the electric field in (V/m) for all MEs.

Band (MHz)	700		800		900		1800		2100		2600		3500	
ME	μ	σ	μ	σ	μ	σ	μ	σ	μ	σ	μ	σ	μ	σ
ME1_P	0.210	0.137	0.395	0.250	0.310	0.206	0.217	0.156	0.154	0.106	0.366	0.255	0.267	0.231
ME2_P	0.174	0.121	0.223	0.121	0.177	0.102	0.177	0.121	0.112	0.057	0.299	0.182	0.210	0.120
ME3_P	0.548	0.317	0.953	0.548	0.506	0.226	0.628	0.408	0.439	0.284	1.113	0.715	0.779	0.518
ME4_P	0.228	0.169	0.373	0.259	0.280	0.176	0.148	0.102	0.135	0.090	0.355	0.248	0.180	0.124
ME5_P	0.436	0.351	0.569	0.478	0.373	0.270	0.218	0.155	0.157	0.100	0.448	0.299	0.149	0.092
ME6_P	0.126	0.096	0.242	0.148	0.238	0.128	0.278	0.206	0.118	0.072	0.480	0.303	0.158	0.132
ME7_P	0.200	0.146	0.386	0.266	0.294	0.230	0.296	0.250	0.181	0.128	0.408	0.324	0.306	0.241
ME8_P	0.313	0.225	0.419	0.265	0.372	0.209	0.171	0.095	0.134	0.076	0.320	0.168	0.318	0.253
ME9_P	0.111	0.062	0.159	0.106	0.121	0.068	0.088	0.060	0.060	0.035	0.118	0.058	0.110	0.094
ME10_P	0.106	0.066	0.289	0.172	0.242	0.149	0.089	0.057	0.100	0.074	0.172	0.095	0.170	0.142
ME11_P	0.358	0.229	0.659	0.524	0.472	0.344	0.373	0.309	0.239	0.174	0.718	0.590	0.224	0.180
ME12_P	0.248	0.101	0.355	0.143	0.301	0.116	0.209	0.081	0.183	0.084	0.422	0.196	0.209	0.111
ME13_P	0.102	0.059	0.186	0.119	0.220	0.175	0.171	0.157	0.088	0.056	0.264	0.202	0.143	0.095
ME14_P	0.173	0.098	0.315	0.211	0.184	0.114	0.139	0.066	0.105	0.059	0.250	0.111	0.130	0.066
ME15_P	0.288	0.162	0.409	0.223	0.401	0.252	0.174	0.092	0.182	0.108	0.347	0.185	0.282	0.195
ME16_P	0.629	0.512	0.597	0.464	0.445	0.337	0.303	0.254	0.292	0.202	0.618	0.458	0.304	0.259
ME17_P	0.016	0.007	0.150	0.102	0.863	0.784	0.284	0.197	0.265	0.244	0.754	0.663	0.052	0.021
ME18_P	0.214	0.088	0.413	0.192	0.307	0.180	0.232	0.115	0.206	0.127	0.696	0.351	0.414	0.373
ME19_P	0.090	0.033	0.142	0.045	0.079	0.022	0.064	0.018	0.055	0.013	0.120	0.039	0.086	0.043
ME20_P	0.301	0.254	0.345	0.269	0.614	0.463	0.227	0.183	0.153	0.140	0.569	0.454	0.039	0.014
ME21_P	0.272	0.112	0.586	0.152	0.466	0.126	0.288	0.083	0.214	0.056	0.850	0.368	0.490	0.195
ME22_P	0.092	0.089	0.102	0.064	0.124	0.072	0.056	0.035	0.080	0.065	0.108	0.058	0.053	0.029
ME23_P	0.240	0.133	0.514	0.381	0.346	0.226	0.242	0.173	0.162	0.095	0.276	0.139	1.108	1.031
ME24_P	0.104	0.118	0.188	0.181	0.144	0.124	0.077	0.066	0.078	0.075	0.203	0.187	0.099	0.078
ME25_P	0.036	0.035	0.156	0.156	0.194	0.170	0.061	0.056	0.046	0.040	0.122	0.106	0.033	0.000
ME26_P	0.161	0.127	0.248	0.170	0.182	0.108	0.103	0.056	0.115	0.071	0.270	0.164	0.193	0.132
ME1_M	0.307	0.267	0.185	0.128	0.113	0.069	0.088	0.066	0.074	0.055	0.191	0.139	0.146	0.119
ME2_M	0.310	0.261	0.309	0.289	0.167	0.136	0.132	0.101	0.161	0.149	0.281	0.247	0.104	0.049
ME3_M	0.079	0.047	0.072	0.032	0.050	0.022	0.038	0.014	0.036	0.017	0.086	0.044	0.094	0.049
ME4_M	0.213	0.180	0.199	0.171	0.219	0.188	0.119	0.102	0.115	0.093	0.210	0.172	0.146	0.118
ME5_M	0.042	0.018	0.141	0.103	0.084	0.059	0.038	0.026	0.058	0.044	0.085	0.062	0.047	0.018
ME6_M	0.036	0.023	0.100	0.067	0.091	0.063	0.033	0.017	0.060	0.049	0.162	0.123	0.061	0.032
ME7_M	0.125	0.095	0.179	0.141	0.083	0.062	0.083	0.074	0.061	0.049	0.130	0.114	0.058	0.030
ME8_M	0.018	0.010	0.030	0.014	0.025	0.013	0.021	0.013	0.017	0.009	0.033	0.015	0.035	0.008
ME9_M	0.417	0.420	0.513	0.512	0.452	0.448	0.143	0.114	0.128	0.088	0.265	0.192	0.156	0.087
ME10_M	0.056	0.015	0.280	0.161	0.215	0.106	0.112	0.072	0.068	0.033	0.291	0.194	0.085	0.049
ME11_M	0.061	0.028	0.207	0.166	0.097	0.067	0.060	0.045	0.048	0.036	0.144	0.103	0.075	0.047
ME12_M	0.025	0.018	0.030	0.016	0.022	0.013	0.018	0.011	0.016	0.009	0.032	0.018	0.034	0.008
ME13_M	0.070	0.048	0.282	0.272	0.184	0.141	0.156	0.130	0.102	0.089	0.294	0.257	0.034	0.003
ME14_M	0.011	0.006	0.031	0.019	0.030	0.020	0.013	0.004	0.016	0.005	0.020	0.007	0.035	0.005
ME15_M	0.084	0.031	0.463	0.170	0.299	0.124	0.175	0.084	0.172	0.053	0.466	0.197	0.112	0.056
ME16_M	0.041	0.009	0.186	0.055	0.104	0.019	0.057	0.018	0.035	0.005	0.236	0.100	0.050	0.009
ME17_M	0.045	0.016	0.092	0.031	0.055	0.017	0.036	0.009	0.055	0.013	0.120	0.035	0.204	0.097
ME18_M	0.074	0.026	0.152	0.052	0.108	0.049	0.058	0.023	0.067	0.022	0.244	0.122	0.199	0.105
ME19_M	0.073	0.050	0.198	0.157	0.169	0.146	0.083	0.074	0.068	0.055	0.183	0.161	0.171	0.127
ME20_M	0.067	0.049	0.129	0.107	0.095	0.083	0.064	0.048	0.054	0.042	0.146	0.127	0.070	0.042
ME1_G	0.015	0.008	0.018	0.010	0.016	0.010	0.008	0.004	0.006	0.002	0.017	0.008	0.033	0.003
ME2_G	0.028	0.013	0.030	0.015	0.032	0.014	0.017	0.008	0.010	0.005	0.043	0.024	0.037	0.004
ME3_G	0.038	0.025	0.033	0.016	0.031	0.012	0.018	0.011	0.010	0.007	0.031	0.015	0.029	0.005
ME4_G	0.012	0.007	0.019	0.011	0.009	0.004	0.007	0.005	0.005	0.002	0.009	0.003	0.032	0.001
ME5_G	0.017	0.005	0.017	0.004	0.014	0.003	0.009	0.002	0.006	0.001	0.022	0.005	0.041	0.003
ME6_G	0.019	0.006	0.015	0.004	0.016	0.005	0.008	0.002	0.005	0.002	0.018	0.006	0.028	0.003
ME7_G	0.098	0.081	0.150	0.143	0.119	0.106	0.050	0.038	0.046	0.039	0.127	0.109	0.078	0.046
ME8_G	0.147	0.156	0.193	0.197	0.139	0.140	0.064	0.057	0.056	0.052	0.128	0.118	0.081	0.064
ME1_B	0.020	0.009	0.031	0.015	0.020	0.007	0.010	0.005	0.010	0.005	0.021	0.010	0.030	0.007
ME2_B	0.079	0.055	0.102	0.069	0.113	0.099	0.046	0.040	0.052	0.040	0.154	0.145	0.052	0.027
ME3_B	0.027	0.010	0.039	0.015	0.027	0.010	0.013	0.005	0.014	0.006	0.026	0.009	0.037	0.006
ME4_B	0.102	0.050	0.132	0.071	0.167	0.081	0.052	0.029	0.057	0.026	0.177	0.095	0.048	0.015
ME5_B	0.018	0.008	0.042	0.018	0.023	0.009	0.006	0.002	0.009	0.003	0.016	0.005	0.036	0.006
ME6_B	0.023	0.008	0.037	0.015	0.021	0.006	0.010	0.004	0.013	0.006	0.025	0.013	0.037	0.008
ME7_B	0.127	0.043	0.164	0.071	0.201	0.068	0.076	0.027	0.083	0.038	0.203	0.063	0.207	0.226
ME8_B	0.032	0.026	0.051	0.048	0.053	0.052	0.027	0.023	0.024	0.022	0.047	0.037	0.139	0.085
ME1_I	0.107	0.090	0.109	0.074	0.173	0.142	0.066	0.055	0.046	0.035	0.107	0.083	0.043	0.006
ME2_I	0.010	0.006	0.022	0.014	0.010	0.002	0.007	0.002	0.009	0.004	0.011	0.002	0.040	0.003
ME3_I	0.022	0.013	0.033	0.014	0.022	0.010	0.014	0.007	0.013	0.007	0.019	0.008	0.039	0.018
ME4_I	0.007	0.004	0.018	0.011	0.009	0.006	0.006	0.003	0.007	0.004	0.011	0.007	0.028	0.003
ME5_I	0.255	0.156	0.258	0.121	0.275	0.097	0.081	0.038	0.095	0.048	0.111	0.053	0.074	0.035
ME6_I	0.081	0.036	0.064	0.023	0.075	0.023	0.023	0.006	0.027	0.010	0.040	0.015	0.030	0.006
ME7_I	0.094	0.077	0.188	0.143	0.159	0.128	0.063	0.045	0.070	0.051	0.130	0.110	0.145	0.150
ME8_I	0.046	0.033	0.041	0.031	0.064	0.039	0.021	0.015	0.020	0.015	0.029	0.019	0.043	0.008

TABLE 4. Median electric field in V/m for all MEs.

| ME \ Band (MHz)	700	800	900	1800	2100	2600	3500
ME1_P	0.137	0.227	0.174	0.101	0.090	0.184	0.096
ME2_P	0.100	0.154	0.108	0.093	0.087	0.202	0.151
ME3_P	0.482	0.797	0.475	0.392	0.291	0.656	0.551
ME4_P	0.115	0.203	0.183	0.093	0.085	0.187	0.105
ME5_P	0.199	0.288	0.227	0.139	0.106	0.294	0.093
ME6_P	0.065	0.172	0.218	0.151	0.090	0.350	0.051
ME7_P	0.101	0.230	0.145	0.118	0.098	0.179	0.136
ME8_P	0.168	0.271	0.242	0.122	0.089	0.229	0.145
ME9_P	0.085	0.088	0.086	0.048	0.045	0.091	0.044
ME10_P	0.066	0.223	0.137	0.062	0.052	0.114	0.068
ME11_P	0.219	0.251	0.210	0.126	0.116	0.215	0.093
ME12_P	0.218	0.295	0.259	0.176	0.161	0.343	0.155
ME13_P	0.067	0.120	0.106	0.065	0.053	0.136	0.082
ME14_P	0.119	0.175	0.128	0.106	0.079	0.210	0.095
ME15_P	0.198	0.268	0.256	0.120	0.117	0.243	0.153
ME16_P	0.217	0.228	0.179	0.086	0.154	0.287	0.119
ME17_P	0.012	0.076	0.277	0.154	0.093	0.273	0.041
ME18_P	0.176	0.328	0.212	0.168	0.137	0.491	0.189
ME19_P	0.077	0.128	0.069	0.056	0.051	0.099	0.063
ME20_P	0.103	0.135	0.265	0.091	0.053	0.257	0.033
ME21_P	0.224	0.550	0.416	0.262	0.200	0.648	0.400
ME22_P	0.015	0.063	0.082	0.031	0.038	0.078	0.033
ME23_P	0.182	0.202	0.177	0.107	0.106	0.246	0.210
ME24_P	0.008	0.040	0.043	0.020	0.019	0.048	0.027
ME25_P	0.008	0.039	0.061	0.018	0.014	0.039	0.033
ME26_P	0.078	0.130	0.112	0.070	0.074	0.163	0.105
ME1_M	0.085	0.105	0.073	0.043	0.036	0.103	0.059
ME2_M	0.117	0.111	0.070	0.060	0.044	0.108	0.077
ME3_M	0.044	0.058	0.039	0.033	0.028	0.060	0.070
ME4_M	0.059	0.061	0.053	0.031	0.034	0.065	0.054
ME5_M	0.034	0.070	0.047	0.023	0.029	0.044	0.038
ME6_M	0.023	0.064	0.048	0.025	0.029	0.083	0.043
ME7_M	0.067	0.086	0.043	0.034	0.030	0.053	0.041
ME8_M	0.011	0.024	0.019	0.013	0.013	0.027	0.032
ME9_M	0.090	0.118	0.085	0.072	0.083	0.130	0.109
ME10_M	0.052	0.192	0.170	0.059	0.050	0.169	0.056
ME11_M	0.047	0.087	0.054	0.030	0.024	0.075	0.049
ME12_M	0.011	0.019	0.012	0.010	0.009	0.018	0.031
ME13_M	0.035	0.078	0.069	0.054	0.035	0.089	0.033
ME14_M	0.008	0.019	0.016	0.011	0.014	0.017	0.033
ME15_M	0.067	0.398	0.248	0.131	0.159	0.375	0.082
ME16_M	0.040	0.174	0.103	0.053	0.034	0.193	0.047
ME17_M	0.038	0.076	0.049	0.032	0.053	0.109	0.161
ME18_M	0.064	0.131	0.084	0.049	0.056	0.178	0.154
ME19_M	0.043	0.071	0.056	0.023	0.024	0.058	0.077
ME20_M	0.038	0.064	0.038	0.036	0.030	0.066	0.044
ME1_G	0.011	0.013	0.010	0.006	0.005	0.014	0.033
ME2_G	0.022	0.021	0.025	0.014	0.008	0.031	0.037
ME3_G	0.026	0.025	0.026	0.012	0.006	0.025	0.027
ME4_G	0.008	0.013	0.007	0.005	0.003	0.008	0.033
ME5_G	0.016	0.016	0.014	0.009	0.006	0.019	0.039
ME6_G	0.018	0.015	0.014	0.008	0.005	0.017	0.027
ME7_G	0.033	0.036	0.039	0.014	0.010	0.029	0.047
ME8_G	0.023	0.039	0.023	0.019	0.016	0.036	0.033
ME1_B	0.017	0.025	0.018	0.009	0.008	0.016	0.027
ME2_B	0.049	0.061	0.044	0.019	0.028	0.050	0.036
ME3_B	0.023	0.035	0.024	0.010	0.011	0.022	0.035
ME4_B	0.072	0.093	0.122	0.036	0.043	0.125	0.041
ME5_B	0.013	0.037	0.021	0.006	0.007	0.015	0.035
ME6_B	0.020	0.030	0.019	0.008	0.009	0.018	0.033
ME7_B	0.026	0.048	0.052	0.023	0.022	0.037	0.039
ME8_B	0.012	0.016	0.014	0.007	0.006	0.016	0.088
ME1_I	0.031	0.067	0.055	0.026	0.023	0.056	0.042
ME2_I	0.007	0.013	0.009	0.006	0.007	0.011	0.039
ME3_I	0.015	0.027	0.018	0.009	0.010	0.015	0.031
ME4_I	0.004	0.011	0.005	0.005	0.005	0.008	0.027
ME5_I	0.172	0.210	0.241	0.062	0.072	0.087	0.055
ME6_I	0.067	0.059	0.070	0.021	0.022	0.032	0.029
ME7_I	0.035	0.082	0.046	0.034	0.033	0.044	0.041
ME8_I	0.028	0.021	0.043	0.009	0.010	0.018	0.039
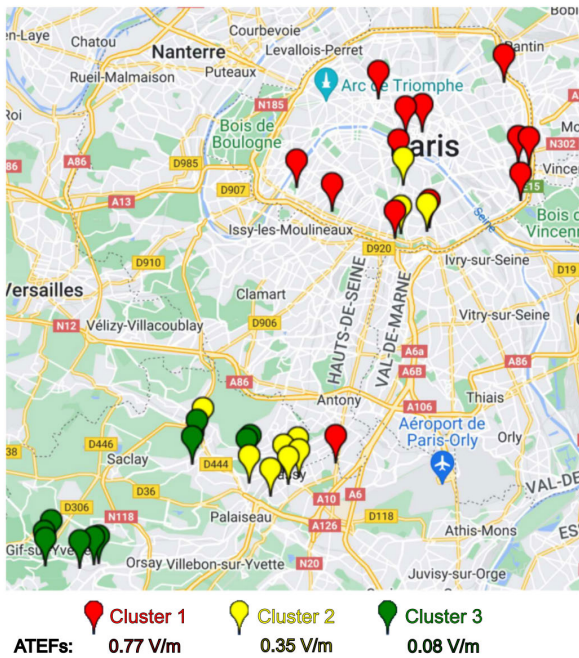
FIGURE 4. Classification of the outdoor measurements into three clusters using the K-Means technique.
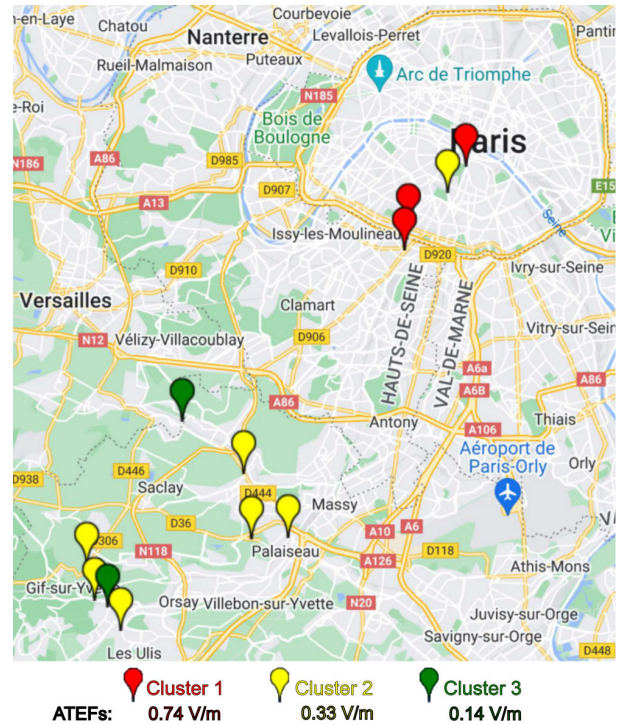

FIGURE 6. Classification of the moving transport MEs into three clusters using the K-Means technique.
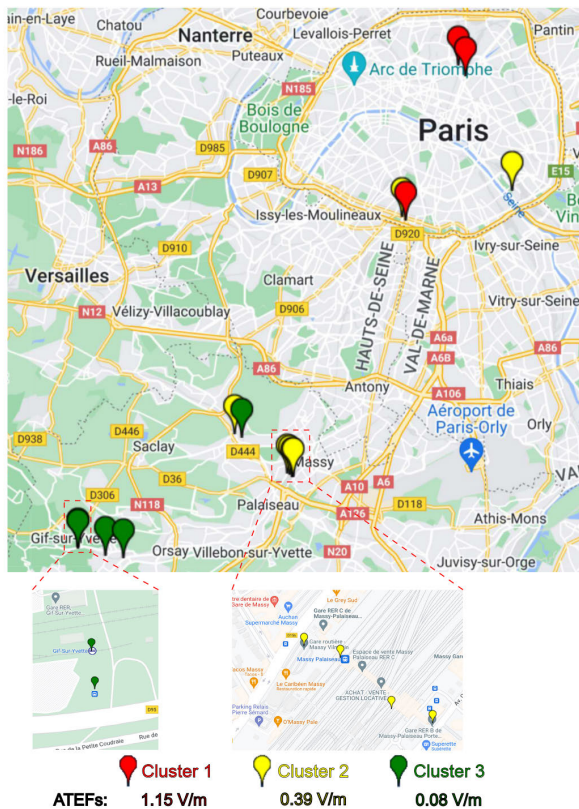

FIGURE 5. Classification of the transport station MEs into three clusters using the K-Means technique.

We also adopt the K-Means to address the clustering of the RF-EMF measurements in the 15 transport stations

MEs, i.e., ME18_**P**, ME19_**P**, ME20_**P**, ME21_**P**, ME22_**P**, ME15_**M**, ME16_**M**, ME17_**M**, ME18_**M**, ME5_**G**, ME6_**G**, ME5_**B**, ME6_**B**, ME5_**I**, ME6_**I**. In Figure 5, we present the results of the K-Means clustering using 3 groups. It is also shown that the exposure levels in Gif-Sur-Yvette, Bures-sur-Yvette, and Igny are similar. The two other clusters are dedicated to Paris and Massy. The ATEFs are 1.15 V/m, 0.39 V/m, and 0.08 V/m for the MEs belonging to the red, yellow and green clusters, respectively. This is generally in adequacy with the nature of environments and population. Some exceptions are also observed here. For example, the exposure level in Bercy metro station in Paris is lower than other MEs in Paris and similar to the exposure level in Massy as this station is located underground.

In addition, we adopt the K-Means to address the clustering of the RF-EMF measurements in the 15 moving transport MEs, i.e., ME_23**P**, ME24_**P**, ME25_**P**, ME26_**P**, ME19_**M**, ME20_**M**, ME7_**G**, ME8_**G**, ME7_**B**, ME8_**B**, ME7_**I**, ME8_**I**. In Figure 6, we present the results of the K-Means clustering using 3 groups. Here, the ATEFs are 0.74 V/m, 0.33 V/m, and 0.14 V/m for the MEs belonging to the red, yellow and green clusters, respectively, where the highest exposure level is observed in Paris. Note that the exposure level inside the moving metro L4 in Paris is lower than in the train, bus, and tram since the coverage is weak underground. It is also observed that trains at Igny and Bures present the lowest exposure level.

In Figure 7, we present the ATEF for different shopping centers located in the considered areas. One can see that the highest level is present at Bercy 2 in Paris (i.e., ME17_**P**).
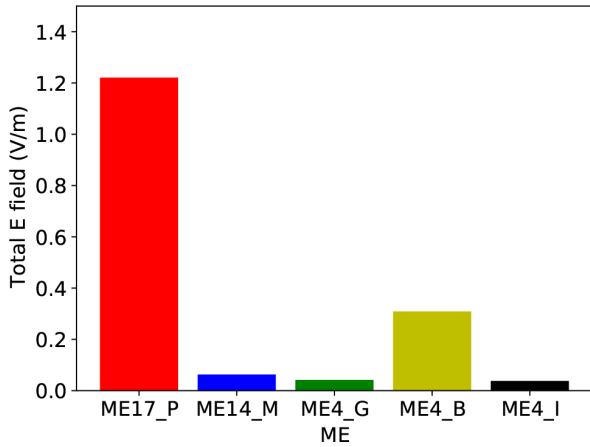
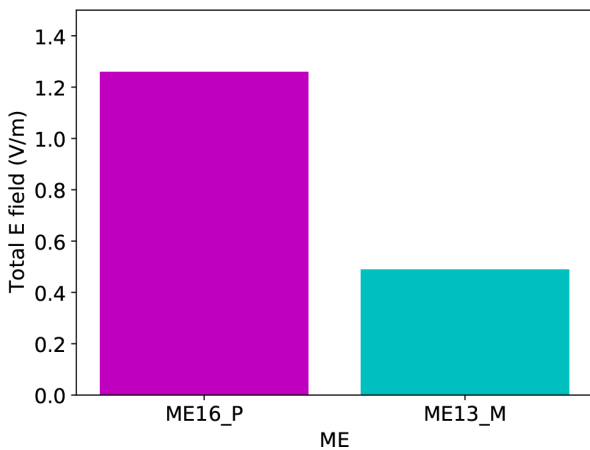**FIGURE 7.** ATEF for different shopping centers.

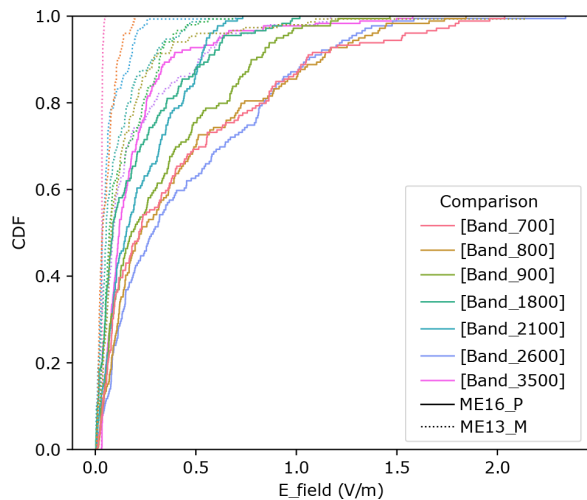
FIGURE 8. ATEF for different universities.

FIGURE 9. CDFs of all considered frequency bands for different universities.

In fact, the ATEF at Bercy 2 is 1.2 V/m, while the ATEF values are less than 0.34 V/m at the other locations.

Figure. 8 shows the ATEF inside two different universities. The results show that the exposure level is higher at Paris University (i.e., ME16_**P**) than at the one located in Massy

(i.e., ME13_**M**). To confirm this result, we plot in Figure 9 the cumulative distribution functions (CDFs) of all considered bands for these two universities. It is clearly shown that the E field is higher at the university located in Paris for all considered frequency bands.

IV. CONCLUSION
This paper presents an EMF DL exposure assessment study in 70 MEs in France located in five study areas based on population density covering one large city, one smaller city, and three village/rural areas. To this end and in accordance with the GOLIAT protocol, the personal ExpoM-RF4 dosimeter is held in a backpack to perform the measurements in different MEs. Thereafter, a correction approach is proposed that is mainly based on comparing the measurements given by ExpoM-RF4 measurements based on reference measurements performed using the Tektronix RTSA far from the body. This approach allows to determine the correction coefficients that are used to correct the measurements across all MEs for each frequency band. A comparison of several MEs with various RF bands is conducted using metrics like quadratic mean, standard deviation, and median of the E field. RF-EMF exposure levels were found to be well below the ICNIRP prescribed limit for all MEs. To group the MEs with similar exposure levels, we also conducted clustering analyses using the K-Means method. The results have shown that the highest exposure level is observed in MEs located in Paris. This can be explained by the important number of antennas deployed in that area to serve the huge amount of users. We also observed that the exposure level in Massy is higher than the ones in the considered villages (Igny, Bures-sur-Yvette and Gif-Sur-Yvette). Some exceptions are seen confirming the presence of heterogeneous environments in the vicinity of some areas. For example, the results have shown that three MEs in Paris among fifteen have an exposure level similar to Massy MEs in outdoor areas. Future work will consist of extending the analyses of measurements in different MEs that are carried out in different EU countries. Another important research axis is related to the characterization of the UL exposure. Note that the assessment of UL power emission involves the utilization, for instance, of Nemo or Qualipoc systems, which are "trace mobile" solutions offered by Keysight and Rohde & Schwarz companies, respectively. These systems employ specialized software installed on mobile phones to capture communication data, including emitted power, frequency utilization, and throughput. Notably, the UL power averaged over time is not directly provided by the trace mobile solutions. Consequently, assessing this metric requires a specific process dependent on the software employed by the trace mobile system. The dedicated measurement protocol and the analyses of UL measurements is planned for future investigation.

REFERENCES

[1] W. B. Chikha, M. Masson, Z. Altman, and S. B. Jemaa, "Radio environment map based inter-cell interference coordination for massive-MIMO systems," *IEEE Trans. Mobile Comput.*, early access, Nov. 17, 2022, doi: 10.1109/TMC.2022.3222763.

[2] S. Aerts, K. Deprez, L. Verloock, R. G. Olsen, L. Martens, P. Tran, and W. Joseph, "RF-EMF exposure near 5G NR small cells," *Sensors*, vol. 23, no. 6, p. 3145, Mar. 2023.

[3] TNS. (2010). *Opinion Social Eurobarometer 73.3, Electromagnetic Fields*. Accessed: Feb. 3, 2023. [Online]. Available: https://europa.eu/eurobarometer/screen/home

[4] *Baromètre Du Numérique*. Accessed: Dec. 12, 2022. [Online]. Available: https://www.economie.gouv.fr/files/files/directions_services/cge/barometre-numerique-2022.pdf?v=1684931616

[5] W. B. Chikha, S. Wang, and J. Wiart, "An extrapolation approach for RF-EMF exposure prediction in an urban area using artificial neural network," *IEEE Access*, vol. 11, pp. 52686–52694, 2023.

[6] B. A. Mulugeta, S. Wang, W. Ben Chikha, J. Liu, C. Roblin, and J. Wiart, "Statistical characterization and modeling of indoor RF-EMF down-link exposure," *Sensors*, vol. 23, no. 7, p. 3583, Mar. 2023.

[7] S. Wang, W. B. Chikha, Y. Zhang, J. Liu, E. Conil, O. Jawad, L. Ourak, and J. Wiart, "RF electromagnetic fields exposure monitoring using drive test and sensors in a French city," in *Proc. 35th Gen. Assem. Scientific Symp. Int. Union Radio Sci. (URSI GASS)*, Aug. 2023, pp. 1–4.

[8] ICNIRP, "Guidelines for limiting exposure to time-varying electric, magnetic, and electromagnetic fields (up to 300 GHz)," *Health Phys.*, vol. 118, no. 5, p. 483, 2020.

[9] *Exposure To Electromagnetic Fields (EMF) and Health*. Accessed: Dec. 12, 2022. [Online]. Available: https://ec.europa.eu/info/funding-tenders/opportunities/portal/screen/opportunities/topic-details/horizon-hlth-2021-envhlth-02-01

[10] *5G ExpOsure, CausaL Effects, and RIsk Perception Through Citizen EngAgemenT (Goliat) Project*. Accessed: Dec. 12, 2022. [Online]. Available: https://projectgoliat.eu/

[11] World Health Organization. *Radio Frequency (RF) Fields Research Agenda*. Accessed: Dec. 12, 2022. [Online]. Available: http://www.who.int/peh-emf/research/

[12] *ExpoM-RF4: User Manual, Fields at Work*. Accessed: Dec. 12, 2022. [Online]. Available: https://fieldsatwork.ch/uploads/Downloads/ExpomRF4/Expom-RF4_Manual_v6.0.pdf

[13] J. F. B. Bolte, "Lessons learnt on biases and uncertainties in personal exposure measurement surveys of radiofrequency electromagnetic fields with exposimeters," *Environ. Int.*, vol. 94, pp. 724–735, Sep. 2016.

[14] S. Tsuruga, K. Yamazaki, A. Ikeda-Araki, C. Miyashita, N. Tamura, R. Kishi, T. Hikage, and K. Sugimura, "Human body shadowing effect on measurement of personal RF exposure meter for epidemiological research on children's health," in *Proc. 35thth URSI Gen. Assem. Scientific Symp.*, 2023.

[15] R. Aminzadeh, A. Thielens, A. Bamba, L. Kone, D. P. Gaillot, M. Lienard, L. Martens, and W. Joseph, "On-body calibration and measurements using personal radiofrequency exposimeters in indoor diffuse and specular environments," *Bioelectromagnetics*, vol. 37, no. 5, pp. 298–309, Jul. 2016.

[16] A. Thielens, S. Agneessens, L. Verloock, E. Tanghe, H. Rogier, L. Martens, and W. Joseph, "On-body calibration and processing for a combination of two radio-frequency personal exposimeters," *Radiat. Protection Dosimetry*, vol. 163, no. 1, pp. 58–69, Jan. 2015.

[17] J. F. B. Bolte, G. van der Zande, and J. Kamer, "Calibration and uncertainties in personal exposure measurements of radiofrequency electromagnetic fields," *Bioelectromagnetics*, vol. 32, no. 8, pp. 652–663, Dec. 2011.

[18] R. Aminzadeh, A. Thielens, S. Agneessens, P. Van Torre, M. van den Bossche, S. Dongus, M. Eeftens, A. Huss, R. Vermeulen, R. de Seze, P. Mazet, E. Cardis, H. Rogier, M. Röösli, L. Martens, and W. Joseph, "A multi-band body-worn distributed radio-frequency exposure meter: Design, on-body calibration and study of body morphology," *Sensors*, vol. 18, no. 1, p. 272, Jan. 2018.

[19] K. Kalliola, K. Sulonen, H. Laitinen, O. Kivekas, J. Krogerus, and P. Vainikainen, "Angular power distribution and mean effective gain of mobile antenna in different propagation environments," *IEEE Trans. Veh. Technol.*, vol. 51, no. 5, pp. 823–838, Sep. 2002.

[20] J. Wiart, *Radio-frequency Human Exposure Assessment: From Deterministic To Stochastic Methods*. Hoboken, NJ, USA: Wiley, 2016.

[21] J. Krogerus, J. Toivanen, C. Icheln, and P. Vainikainen, "Effect of the human body on total radiated power and the 3-D radiation pattern of mobile handsets," *IEEE Trans. Instrum. Meas.*, vol. 56, no. 6, pp. 2375–2385, Dec. 2007.

[22] Tektronix. *Spectrum Analyzer RSA306B USB Real Time Spectrum Analyzer Datasheet*. Accessed: Dec. 12, 2022. [Online]. Available: https://download.tek.com/datasheet/RSA306-USB-Spectrum-Anayzer-Datasheet-37W307676.pdf

[23] *Microwave Vision Group*. Accessed: Dec. 12, 2022. [Online]. Available: https://www.mvg-world.com/fr

[24] X. Wu, V. Kumar, J. R. Quinlan, J. Ghosh, Q. Yang, H. Motoda, G. J. McLachlan, A. Ng, B. Liu, and P. S. Yu, "Top 10 algorithms in data mining," *Knowl. Inf. Syst.*, vol. 14, no. 1, pp. 1–37, 2008.

[25] Z. Huang, "Extensions to the k-means algorithm for clustering large data sets with categorical values," *Data Mining Knowl. Discovery*, vol. 2, no. 3, pp. 283–304, 1998.

WASSIM BEN CHIKHA (Senior Member, IEEE) received the Engineering degree in computer science from the National Engineering School of Sfax, Tunisia, in 2012, and the Ph.D. degree in electronic and technology of information and communication from the Tunisia Polytechnic School, in 2017. From 2017 to 2020, he was a Postdoctoral Researcher with the University of Udine, Italy, in close collaboration with STMicroelectronics Company. His research included IoT sensors for STM32 open development environment low-power applications using the Contiki operating system. From 2020 to 2021, he worked on radio network management using artificial intelligence (AI) as a Postdoctoral Researcher with the Orange Laboratories. He is currently a Research and Development Engineer with Telecom Paris, IP Paris, France. His current research interest includes the application of AI in the assessment of electromagnetic field exposure.
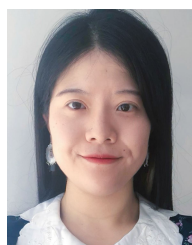
YARUI ZHANG received the B.E. degree from the School of Electronic Engineering, Xidian University, Xi'an, China, in 2018, and the M.S. degree in control, signal, and image processing and the Ph.D. degree in signal and image processing from Université Paris-Saclay, Gif-sur-Yvette, France, in 2019 and 2023, respectively. Her research interests include inversion and imaging, signal and image processing, and inverse scattering problems.

JIANG LIU received the B.S. degree from the University of Electronic Science and Technology of China (UESTC), Chengdu, China, in 2014, the master's degree from the National Key Laboratory of Science and Technology on Communications, and the Ph.D. degree from the Laboratory of Signals and Systems, Paris-Saclay University, Paris, France, in 2022. His research interests include wireless communications and communication theory, with a particular focus on signal detection of wireless communication systems.

SHANSHAN WANG (Member, IEEE) was born in Nanjing, China, in 1991. She received the B.Sc. degree in communications engineering from Soochow University, Suzhou, China, in 2013, the M.Sc. degree (Hons.) in wireless communication and signal processing from the University of Bristol, Bristol, U.K., in 2014, and the Ph.D. degree from the Laboratory of Signals and Systems, Paris-Saclay University, Paris, France, in 2019. From 2015 to 2018, she was with the French National Center for Scientific Research (CNRS), Paris, as an Early Stage Researcher of the European-Funded Project H2020 ETN-5Gwireless. Her research interests include stochastic geometry, EMF exposure, and machine learning for applications in wireless communications. She is currently a Postdoctoral Researcher with Telecom Paris, IP Paris, France. She was a recipient of the 2018 INISCOM Best Paper Award. She served as a Guest Editor for the *Sensors* (MDPI), in 2022.

SRIKUMAR SANDEEP received the M.S. and Ph.D. degrees in electrical engineering from the University of Colorado Boulder, in 2011 and 2012, respectively.

He was a Postdoctoral Researcher with the University of Colorado Boulder, in 2013, focusing on antenna design and École Polytechnique, Montreal, in 2016, where worked on metasurfaces. This was followed by research scientist appointments with the Singapore University of Technology and Design (SUTD), Norwegian University of Science and Technology (NTNU), and Telecom Paris. His research interests include computational electromagnetics, antenna design, metasurfaces, signal integrity, wireless power transfer, high performance computing, bioelectromagnetics, and applied machine learning. He is noted for his work on computational electromagnetics applied to metasurfaces. He is unique in the sense that he is an expert in finite difference time domain (FDTD) method and method of moments (MoM). He had reviewed papers for several international journals, such as *Applied Optics*, Applied Computational Electromagnetic Society, IEEE Transactions on Geoscience and Remote Sensing, and IEEE Antennas and Propagation Letters. He has authored more than 20 publications and is a co-inventor of a U.S. patent.

MÒNICA GUXENS received the Ph.D. degree, in 2008. She is currently pursuing the Medical Doctor degree in preventive medicine and public health. She is also a Research Professor and the Head of the BrainChild Laboratory, Barcelona Institute for Global Health (ISGlobal). Her research interests include the role of environmental factors, including electromagnetic fields, on children's development, in particular on brain development. She is also the Director of the Spanish INMA Project, a multi-site birth cohort. She has been leading several projects RF-EMF and health. She is also coordinating the large Horizon Europe Project GOLIAT "5G exposure, casual effects, and risk perception through citizen engagement."

ADRIANA FERNANDES VELUDO was born in Lisbon, Portugal, in 1993. She received the M.Sc. degree in veterinary medicine from the University of Lisbon, in 2018, and the M.Sc. degree in one health from Utrecht University, The Netherlands, in 2021. She is currently pursuing the Ph.D. degree in epidemiology with the Swiss Tropical and Public Health Institute, Basel, Switzerland, which main focus will be to characterize RF-EMF exposure from legacy and newly introduced mobile phone technologies.

MARTIN RÖÖSLI received the M.Sc. degree in environmental science from the Swiss Federal Institute of Technology in Zürich (ETHZ), in 1997, and the Ph.D. degree in epidemiology from the University of Basel, in 2001. He is currently a Professor in environmental epidemiology with the Swiss Tropical and Public Health Institute in Basel and leads the Environmental Exposures and Health Unit. His research interests include environmental health topics including ionizing and non-ionizing radiation, transportation noise, climate change, pesticides, passive smoking, and ambient air pollution. He is conducting exposure assessment studies, aetiological research, and health impact assessments. He is also a member in various national and international commissions on environmental health risks, including BERENIS (Swiss Expert Group on Non-Ionising Radiation), ICNIRP, the Scientific Council on Electromagnetic Fields of the Swedish Radiation Safety Authority, and Scientific Council of the European Bioelectromagnetics Association EBEA (2009 and 2017). He has published numerous scientific articles, reviews, and book chapters.

WOUT JOSEPH (Senior Member, IEEE) was born in Ostend, Belgium, in October 1977. He received the M.Sc. degree in electrical engineering from Ghent University, Belgium, in July 2000, and the Ph.D. degree, in March 2005. This work dealt with measuring and modelling of electromagnetic fields around base stations for mobile communications related to the health effects of the exposure to electromagnetic radiation. From 2007 to 2012, he was a Postdoctoral Fellow of the Research Foundation—Flanders (FWO-V). Since October 2009, he has been a Professor in the domain of "Experimental characterization of wireless communication systems." He has been an IMEC PI, since 2017. His research interests include electromagnetic field exposure assessment, propagation for wireless communication systems, antennas, and calibration. Furthermore, he specializes in wireless performance analysis and quality of experience.

JOE WIART (Senior Member, IEEE) received the Engineering (Diploma) degree in telecommunication, in 1992, the Ph.D. degree, in 1995, and the H.D.R. degree, in 2015. Since 2015, he has been the Holder of the Chair C2M "Caractérisation, Modélisation et Maîtrise of the Institut Mines Telecom," Telecom Paris. His works gave rise to more than 150 publications in journals and more than 200 communications. His research interests include experimental, numerical methods, machine learning, statistic applied in electromagnetism, dosimetry, and exposure monitoring. He has been an Emeritus Member of The Society of Electrical Engineers (SEE), since 2008. He is also the Chairperson of the TC106x of the European Committee for Electrotechnical Standardization (CENELEC) in charge of EMF exposure standards. He is also the past Chairperson of the International Union of Radio Science (URSI) Commission k and has been the Chairperson of the French Chapter of URSI.

• • •